Microgrid for Radio Access Network Resilience

Microgrid for Radio Access Network Resilience

Greta Vallero
Department of Electronics and Telecommunications
Politecnico di Torino, Italy
Email: greta.vallero@polito.it

Michela Meo
Department of Electronics and Telecommunications
Politecnico di Torino, Italy
Email: michela.meo@polito.it

***Abstract*—The consistent growth in electricity demand, coupled with factors such as political instability, cyberattacks, and the rising frequency of natural disasters due to the climate crisis, poses challenges to the reliability and consistency of the power grid supply. The malfunctioning of the power grid, in turn, has a cascading effect on the communication infrastructure, which heavily relies on the stability of the electricity grid. Despite this, enhancing the resilience of computing and communication facilities is fundamental. Their crucial role in supporting essential aspects of our daily lives requires ensuring their continuous and dependable operation. To cope with this, in this work, we view a group of Base Stations (BSs) of a Radio Access Network (RAN) as consumers within a Microgrid (MG), each equipped with a Photovoltaic (PV) Panel and interconnected through dedicated power cables to exchange their generated energy. We introduce a RAN resource and energy management, that, during a Power Grid Outage (PGO), aims at keeping active the most loaded BSs, given the available generated energy within the MG. We evaluate the impact of the number of BSs in the MG, the PV Panel capacity, the duration of the PGOs and the BS traffic shape profiles, formalizing also the required setting which guarantees the efficacy of our methodology. Results reveal that the performance achieved with PV Panels not exceeding 6 kWp is comparable to that of larger PV Panels (up to 12 kWp), if the MG and the RAN resource management are implemented, making our solution feasible in terms of installation space requirements and increasing the hourly served traffic up to 300%.**

***Index Terms*—Resilience, Microgrid, Base Station, Renewable Energy Sources, Power Grid Outage, Radio Access Network.**

I. Introduction

From 2010 to 2022, the number of reported service outages in the communication network has grown by 155% in Europe [1]. In 2021, the lost user hours, the metric for measuring the impact of each service interruption, knows as the number of interruption hours times the involved users, was 5 106 million, at least 2.6 times larger than each year since 2010 [1]. ENISA (European Union Agency for Cybersecurity), in [1], identifies the BSs of the RAN as one of the most network equipment that is affected in these interruptions. Approximately 30% of interruptions are due to failures in the power grid, upon which the communication infrastructure relies. Providing a continuous and high-quality power supply is challenging because of the ever growing electricity demand, political instability, cyberattacks and climate crisis, which makes natural disasters more frequent, limiting power grid operation. Nevertheless, computing and communication facilities have become vital supports for essential utilities in our daily lives. Ensuring their uninterrupted and dependable operation is imperative, extending beyond normal operating conditions. The computing and communication infrastructure must not only be *reliable*, ensuring consistent and dependable performance, and *robust*, capable of sustaining full operation without succumbing to system failures in the face of potential challenges, but also *resilient*. This means that it has to demonstrate the ability to adapt to external changes that may alter system behaviors and swiftly recover after operational interruptions [2].

Typically, in case of energy grid provisioning shortages, devices in the core and backhaul networks that aggregate large amounts of traffic, rely on costly energy batteries as backup power systems. Nevertheless, in the RANs, the situation is more critical, because of the widespread distribution of the BSs of this network. To address this issue, an emerging trend considers the integration of Renewable Energy Sources (RESs), located in proximity of the BSs, for enhancing network resilience. When designed effectively, RESs reduce the network's reliance on the power grid, mitigating the potential cascade impact of PGOs. During the last few years, there has been a huge penetration of these RESs, as demonstrated by the installation of 167 GW of distributed PV Panel systems globally, between 2019 and 2021 [3]. This is in response to the first global energy crisis, responsible for the substantial growth in both gas and coal costs, causing approximately 90% of the rise in electricity expenses worldwide [4]. Meanwhile, the even growing installation of RES is motivated by the need for actions to fight the climate crisis and accomplish the ambitious goal of net zero emissions by 2050 [5]. In this context, the concept of MGs is gaining attention within conventional power grids. MGs are characterized as low-voltage, small-scale electricity grids that encompass a diverse range of distributed RES. These resources can operate in a controlled and coordinated manner to effectively address energy demand [6], [7].

In the literature, powering BSs through RES has been an attractive solution to make the RAN more sustainable and self-sufficient, while reducing also the electricity bill [8]–[11]. Besides the benefits in terms of energy bill, sustainability and self-sufficiency, largely demonstrated in the literature, powering the BSs with RES is a promising solution to mitigate the effect of PGOs on the mobile communication service [12]. Our prior work, presented in [13], demonstrates that the utilization of a PV Panel as an energy backup system efficiently alleviates the impact of PGOs on mobile communication services.

This paper aims at enhancing the RAN resilience in case of PGO, by grouping the BSs in MGs. These MGs leverage dedicated power cables to exchange energy, generated by PV Panels installed in the BS proximity. We design an ad-hoc RAN resource and energy management, that, in case of PGO, keeps active the most loaded BSs, until the MG generates sufficient energy, to maintain continuous communication service, thereby improving RAN resilience. Our analysis indicates that our proposed methodology is promising, demonstrating an increasing of the hourly served traffic load during a PGO up to 300%. Through simulations, we evaluate how the number

of BSs within the MG, the capacity of the PV Panel, the duration of PGOs and the traffic shape profiles of the BSs impact the Quality of Service (QoS) in the RAN during a PGO. Additionally, our work formalizes the necessary configuration to ensure the effectiveness of our approach.

The paper is organised as follows. Section II reviews related works, while section III describes the scenario and our proposed methodology. In section IV, we present and discuss the results of our simulations and the conclusions are drawn in section V.

II. State of the Art

According to the work presented in [2], effective system design requires significant attention to both robustness and resilience. While robustness refers to the system's ability to maintain or restore its performance and operation despite facing challenges and disruptions, resilience goes further, incorporating the ability to restore operations after unanticipated events that violate design assumptions. With the growing reliance on communication services and the imperative need for uninterrupted connectivity, robustness and resilience have become critical in communication networks. In [2], authors evaluate system robustness and resilience through anticipation, absorption, adaptation, and rapid recovery from adverse events. Authors in [14], [15] ensure network reliability, availability, and robustness by implementing measures and protocols that leverage hardware redundancy and diversity to minimize single points of failure, ensure network scalability to accommodate potential future growth in traffic demand without overloading the network, implement traffic re-routing, load balancing, interference management and security measures to prevent congestion and detect malicious attacks. The work presented in [16] highlights the importance of power autonomy and response in case of disaster to enhance resilience in the power supply for telecommunication networks.

Typically, network infrastructure is equipped with an energy battery backup system to cope with the lack of energy supply during temporary electric grid interruptions, which may cause communication network outages. However, these battery backup systems are costly and require significant space for placement and periodic maintenance. For this reason, in [17], the battery backup system of a BS is replaced by a diesel generator. In [18], authors use electrical vehicles as mobile energy batteries to transport energy where needed and restore energy supply in emergencies. A new trend to improve network resilience involves the employment of RES. The penetration of RES in RAN has been introduced to improve network sustainability and reduce Operational costs (OPEX) [9], [10], [19], [20]. When these RES operate in a controlled and coordinated manner, they form a MG that can effectively address the energy requirements of remote areas and emergency situations [21]. Additionally, as demonstrated in our previous work in [13], properly designed RES for supplying RANs may be effective in reducing dependency on the power grid, thereby preventing cascade effects of power grid outages.

While these works introduce promising solutions for improving RAN sustainability and reducing OPEX, they do not tackle RAN resilience. To overcome this limitation, we evaluate this aspect and propose a solution that groups RAN BSs into a MG, managing RAN resources in the event of a PGO according to available energy generated by PV Panels, installed in the BS proximity.

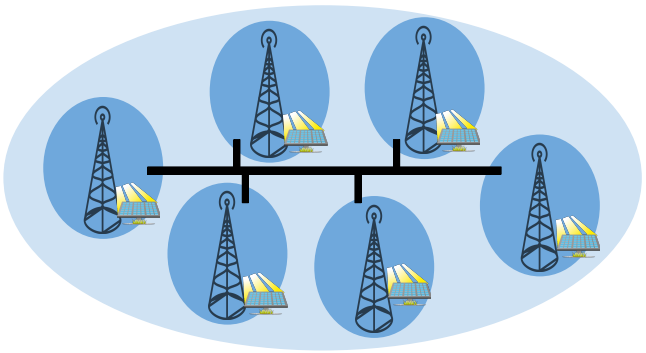

Fig. 1. The portion of RAN under consideration: it is composed of N BSs, forming a MG, that act as the loads and the distributes RESs within the MG, transferring the produced energy through dedicated cables.

TABLE I
BS LINK BUDGET PARAMETERS [22], [23].

Parameter	**2100 MHz**
Frequency (MHz)	2100
Bandwidth (MHz)	120
Used Subcarries	7680
Total Subcarries	12288
Sampling Factor	1536
TDD Duty Cycle DL (%)	75
TDD Duty Cycle UL (%)	25
Spatial Duty Cycle (%)	0
BS Transmit Antenna Gain (dBi)	18
BS Transmit Array Antenna Feed Loss (dBi)	2
BS Ratiated Power (dBm)	49
BS Number of Antenna Elements	1
User Antenna Element Gain (dBi)	0
User Transmit Power (dBm)	23
User Antenna Height (m)	1.5
User Number of Antenna Elements	1
Receiver Noise Figure (dB)	8

III. Methodology

In this Study, we focus on a subset of a RAN, comprising N BSs, forming a MG, as illustrated in Fig. 1. These BSs act as the loads and the distributes RESs within the MG, transferring energy through dedicated cables, see black lines in Fig. 1. Each BS operates on 5G technology, with a frequency of 2.1 GHz and a maximum channel bandwidth of 120 MHz. The link budget details are summarized in Table I [23]. Each BS is equipped with a PV panel system, which provides the energy for its supply. We assume a crystalline silicon technology for the PV modules and consider a DC-to-AC inverter efficiency of 96%. Given optimal tilting and azimuth angles for the location (20° and 180°, respectively), an average daily solar radiation of 4 kWh/m^2 is observed throughout the year, accounting for typical performance losses of approximately 14% in real systems.

At each one-minute time slot, the total energy produced in the MG, $E_p^{(t)}$, is calculated as $\sum_{i=1}^{N} E_{p,i}^{(t)}$, where $E_{p,i}^{(t)}$ represents the energy produced by the PV panel of the *i-th* BS in the MG at time t. Similarly, the total energy demand in the MG at time t, $E_c^{(t)}$, is computed as $\sum_{i=0}^{N} E_{c,i}^{(t)}$, where $E_{c,i}^{(t)}$ denotes the energy consumed by the *i-th* BS in the MG at time t. The BSs of a MG exchange energy through dedicated cables, to maximise the usage of the produced renewable

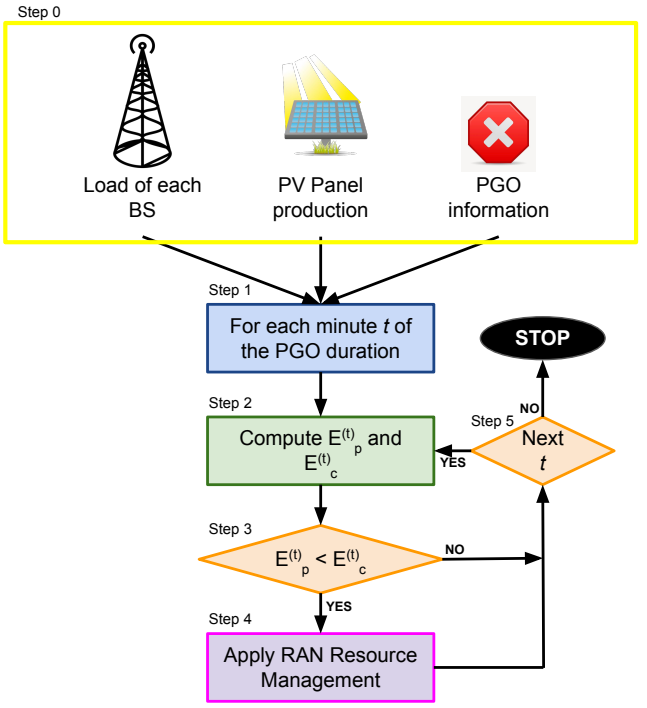

Fig. 2. Flow chart with the different steps of our simulations.

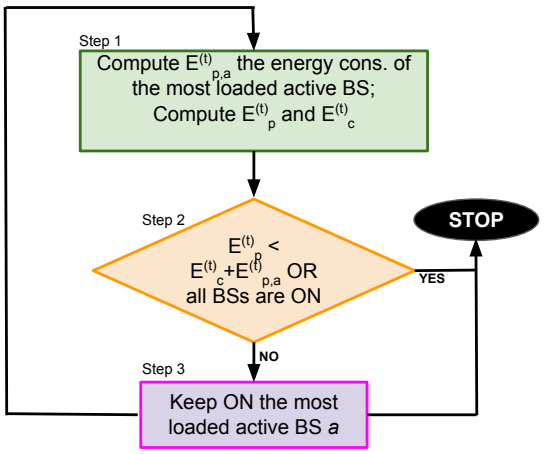

Fig. 3. Different steps of the RAN Resource Management.

energy. The losses along the power cables are negligible due to the relatively short range distances considered in this context [24]. In normal operating conditions, in case the produced energy is not enough for the MG supply, i.e. $E_p^{(t)} < E_c^{(t)}$, the missing energy is drained from the power grid. When a PGO occurs, the considered portion of RAN can not draw energy from the power grid, but it relies only on the energy that is produced by the PV Panels within the MG. In this situation, if that amount of energy is insufficient for the BS supply, i.e. $E_p^{(t)} < E_c^{(t)}$, some or all of the BSs shut down, and the service they provide is interrupted. To make the portion of RAN as resilient as possible from PGOs, we propose a RAN resource and energy management. Its objective is the maximization of the available RAN capacity, determining which BSs are powered by the available energy. Details of the RAN resource and energy management are given in the following.

To evaluate the resilience of the considered portion of the RAN using our proposed methodology, we develop a simulation-based ad hoc framework. Each simulation begins at the beginning of a PGO and continues for its entire duration. The framework takes as input the load on each BS in the MG, the date and duration of the PGO, and the PV panel production during that period (see step 0 in Fig. 2). Using a one-minute granularity, the produced and consumed energy are computed (step 1 in Fig.2). Subsequently, the RAN resource and energy management is applied if $E_p^{(t)} < E_c^{(t)}$, i.e. if there is not enough energy for supplying all the BSs (steps 3 and 4 in Fig.2). The simulation concludes upon the termination of the PGO (step 5 in Fig. 2).

A. The RAN Resource Management

As previously mentioned, each simulation begins with the start of a PGO, which persists for its entire duration. Throughout the PGO period, the section of the RAN under consideration is unable to access energy from the power grid and relies solely on the energy generated by the PV Panels installed on each BS. This means that when the produced energy is not sufficient for the considered portion of RAN, i.e. $E_p^{(t)} < E_c^{(t)}$, part or all the BSs can not be powered and de-activate, interrupting the service they provide. Managing the available and deciding which BSs should be powered through the available energy, while maximizing the amount of traffic that can be carried, leads to a computational problem known as the Knapsack problem, which is classified as NP-Hard. We implement a greedy approach that determines which BSs are powered and provide the service, given the available energy. Specifically, we arrange the BSs in descending order of load, from the most to the least loaded, and iteratively we keep active BS a (step 2 in Fig. 3), if the generated energy is sufficient for the MG supply, i.e., $E_p^{(t)} \geq E_c^{(t)} + E_{p,a}^{(t)}$, where $E_c^{(t)}$ considers only the active BSs within the MG (step 3 in Fig. 3) and $E_{p,a}^{(t)}$ is the energy consumption of BS a. The sorting is performed in descending order of load because less loaded BSs are less energy-efficient than highly loaded ones. This implies that the energy required to transmit a unit of traffic, measured in *J/bit*, is lower for highly loaded BSs compared to less loaded ones [25].

B. Input data

Traffic data: In our study, we use traffic data provided by a large Italian Mobile Network Operator (MNO). The data report the hourly load at more than 1,400 BSs, in the city of Milan and in a wide area around it, for a duration of two months in 2015. We scale the data, to keep track of the growth of the mobile traffic demand market in Italy from 2015 to nowadays, using a factor equal to 27.6, as reported in [26], [27]. In our work, each BS is associated with one of these traces. For each of them, the typical day is computed, as the hourly average among the different days of the trace.

Energy outage data: For this work, we use data about more than 3,000 outages, presented in [13]. They are collected using an api confidentially provided by an Italian Distribution System Operator (DSO). Given the year and the ID of an energy meter, it returns the outages that occurred during that year, which involved that user terminal. Each record reports the location, the duration and the starting time of an outage. Data from 2014 to 2018, in the city of Turin, Italy, are

TABLE II
POWER REQUIREMENT MODEL PARAMETERS [22], [23], [30].

Parameters	Explanation	Values
P_T (W)	Radio frequency transceiver power	1.5
η	Efficiency of the power amplifier	0.5
P_B (W)	BH power link	10
P_C (W)	Cooling system power	200
P_R (W)	Rectifier power	50
P_{DSP} (W)	Digital signal processing power	1
N_A	Number of antenna sectors	1

collected for our study. Information about users, e.g., energy meters, spread over the whole city are collected in order to have representative data for the considered urban area.

Energy production data: The data of the PV panel production in Milan are taken from the PVWATT tool[1], see [28]. This tool provides data derived from realistic solar irradiation patterns, representing the typical meteorological conditions for the area over the course of a year. The data, available at hourly intervals, incorporate the main losses experienced in a real PV system during the conversion of solar radiation into electricity. Thus, the dataset reports the hourly electricity production of PV panels in Milan, Italy, over the course of a year.

C. Scenarios

To generate the MGs, we utilize a clustering approach where each data point corresponds to the hourly load during the typical day associated with a BS from the dataset discussed above. Specifically, we apply balanced clustering, outlined in [29], which maintains a cluster size constrained to match the predetermined size of each MG denoted as N. We explore two different scenarios for generating the MGs as follows.

Homogeneous MG (HomMG): This well represents the hypothesis of the homogeneity of the loads in close geographical areas. In order to generate the different MGs, we use a clustering technique based on the traditional k-means approach: it iteratively assigns clusters to the nearest one, if this does not violate the maximum cluster size.

Heterogeneous MG (HetMG): This reflects the scenario of an area characterized by heterogeneous loads within close geographical proximity, which is typical of areas with hotspots such as tourist attractions or parks. Using our traffic data, which consists of multiple BS traffic demand traces, we employ a customized variation of the k-means approach. In contrast to the traditional method, each iteration assigns a cluster to the furthest point, ensuring that the size of the new cluster does not exceed the maximum cluster size.

D. Power Consumption Model

As in [23], the energy consumption of a BS is computed as:

$$E_c^{(t)} = t\Big(N_a\left(P_t + P_{dsp} + \eta P_a\right) + P_r + P_c + P_{bh}\Big) \quad (1)$$

where N_a is the number of elements of the BS antenna, P_t is the power of the radio frequency transceiver, in W, P_{dsp} is power of the digital signal processing, in W, η is the efficiency of the power amplifier and P_a is the input power of the amplifier unit, in W. P_r, P_c and P_{bh} are the power drained by the rectifier, the cooling system and the backhaul link, respectively, in W. The parameter values are reported in Table II [22], [23], [30].

[1]https://pvwatts.nrel.gov/pvwatts.php

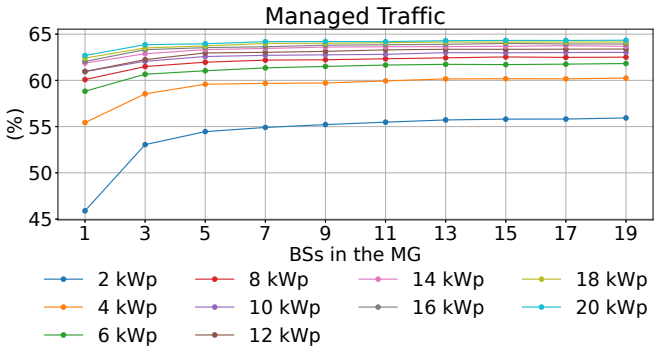

Fig. 4. *Managed Traffic* with RAN resource management varying the PV panel capacity and the number of BSs within the MG.

E. Performance Indicators

Managed Traffic (%): Average percentage of traffic demand that is met by the network during a PGO, since some BSs are inactive and do not provide any service because of the energy supply shortages. This metric serves as an indicator of QoS within the RAN during PGOs.

Active time to outage duration (A2D): Average time share during which the BS remains operational relative to the PGO duration. In the event of a PGO, a BS is considered active and capable of providing service if its PV Panel or the ones of the BSs in its MG produce sufficient energy for its supply. Otherwise, the BS is off and does not provide any service.

IV. EXPERIMENTAL RESULTS

In our simulations, each PGO from our data set is applied to every MG generated as described in section III. The results are presented as averages across the various simulated MGs and PGOs. Unless differently stated, we focus on the *HomMG* scenario.

A. Impact of the number of BSs in the MG

This part of our work analyses the impact of the number of BSs composing the MG and the capacity of the PV Panels. In Fig. 4, each curve in the plot is the percentage of the *Managed Traffic* with different capacity of the PV Panel installed on each BS, varying, on the x-axis, the number of BSs in the MG. From the figure, we observe that the growth of the PV Panel capacity increases the *Managed Traffic* during the PGO, as more energy is produced. Specifically, the *Managed Traffic* is smaller than 56%, in case the capacity of the PV Panel of each BS is 2 kWp while it exceeds 64%, when the capacity is 20 kWp. Additionally, the figure highlights that the rise of the number of the BSs in the MG increases the percentage of the *Managed Traffic*. This happens because when the generated energy is not enough for the MG supply, certain BSs are off and the energy produced by the PV Panel of those off BSs is redistributed and utilized to power the other BSs, that can remain active. The growth of the *Managed Traffic* is significant for small PV Panel systems, accounting for 17.5% with 2 kWp, but it diminishes for large ones: not exceeding 7% in case of PV Panel capacity equal to 8 kWp. Notice that a MG composed of 9 BSs, each equipped with 6 kWp, manages a larger portion of traffic compared to a single BS, equipped with 10 or 12 kWp PV Panel. To better

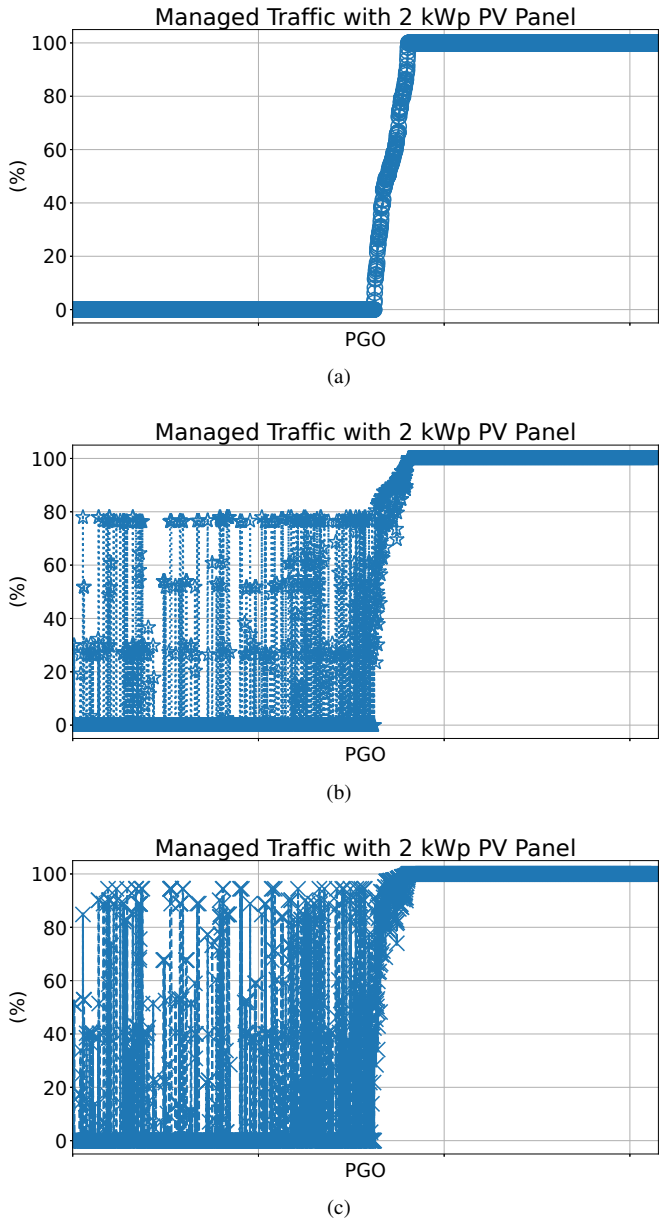

Fig. 5. *Managed Traffic* for each PGO, with a 2 kWp PV Panel, varying the number of BSs within the MG: 1 BS (a), 4 BSs (b) and 16 BSs (c).

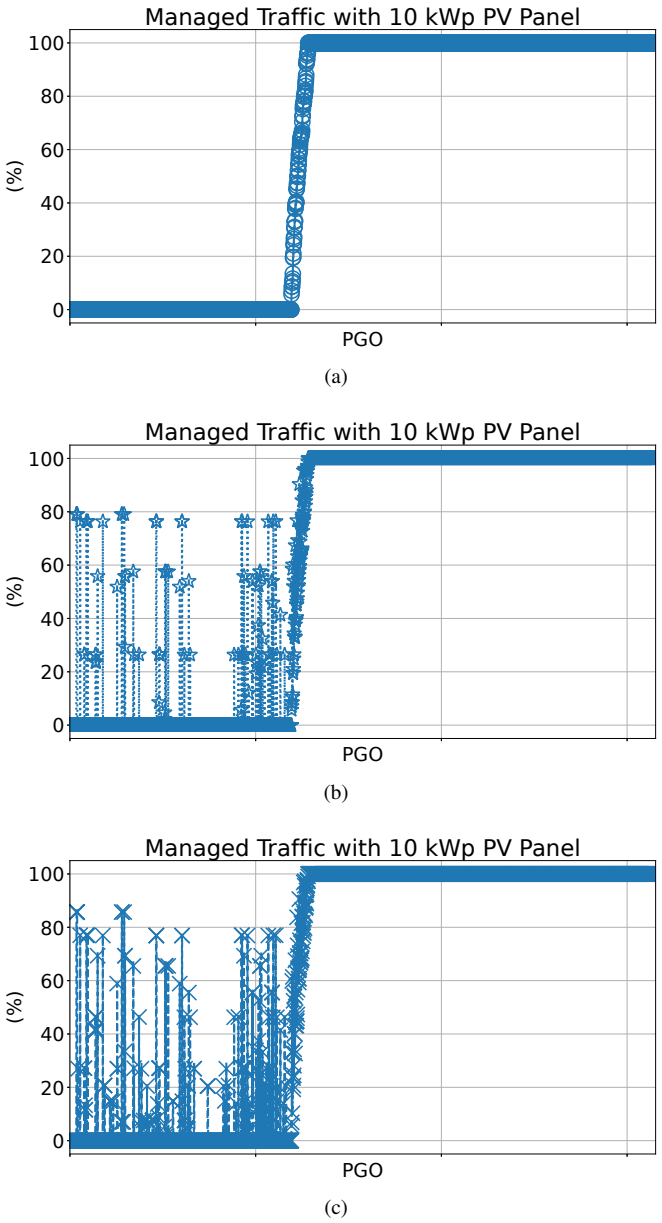

Fig. 6. *Managed Traffic* for each PGO, with a 10 kWp PV Panel, varying the number of BSs within the MG: 1 BS (a), 4 BSs (b) and 16 BSs (c).

catch the effect of the BS number of the MG, Figs. 5a, 5b, and 5c show the percentage of the *Managed Traffic*, for each simulated PGO (x-axis), in case the MG is composed of 1 BS, 4 BSs and 16 BSs, respectively, with PV Panel capacity of 2 kWp. The same is shown in Figs. 6a, 6b, and 6c, respectively, in case the capacity of each employed PV Panel is 10 kWp. From Figs. 5a and 6a, we notice that 43% and 59% of PGOs, respectively, are totally transparent to the provided service, with no loss of traffic when each MG is composed of a single BS. This typically occurs during daily hours. For 51% and 38% of PGOs, respectively, the percentage of *Managed Traffic* is 0%, indicating a total interruption of the service. Furthermore, for the remaining 6% and 3% of PGOs with 2 kWp and 10 kWp-equipped BSs, respectively, the *Managed Traffic* ranges between 0% and 100%. The growth of the number of BSs in the MG increases the *Managed Traffic*, as seen in Figs. 5b, 5c, 6b, 6c. Now, we focus on the PGOs which cause traffic loss when the MG is composed of a single BS, i.e. for which the *Managed Traffic* is lower than 100%, as these are the instances where QoS needs improvement. Among these, the growth in the MG size increases the *Managed Traffic* in 32% and 38% of PGOs, for MG composed of 4 and 16 BSs, respectively, with 2 kWp-equipped BSs. For 22% and 23% of these instances, the network is able to manage at least 50% of the traffic demand. Results if the BSs are equipped with a 10 kWp PV Panel are similar, but with slightly less sensitivity to the MG size variation. Focusing on PGOs with *Managed Traffic* lower than 100% with single BS MGs, the *Managed Traffic* improves in 10% and 20% of cases, when the MG size is 4 and 16 BSs, respectively. Additionally, among these PGOs, it is larger than 50% in 9% of cases.

Now, we analyse the impact of the MG size, during the different hours of the day. In Fig. 7, the *Managed Traffic* is plotted, when the PV Panel of each BS is 2 kWp and 10 kWp, in blue and orange, respectively, varying the number of BSs in the MG, denoted by different markers. Each point of the curves in the figure is the *Managed Traffic*, computed considering only the PGOs that start at the corresponding hour, which varies on the x-axis. From the figure, we identify

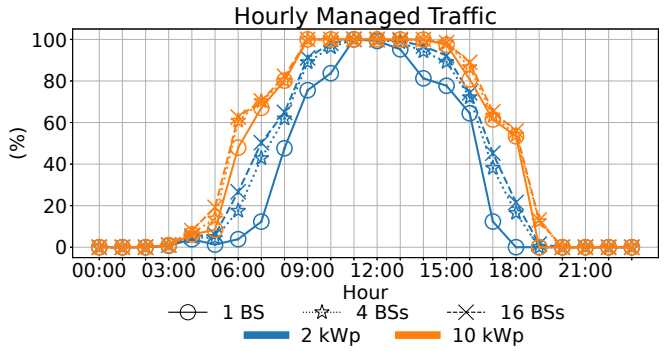

Fig. 7. Hourly Managed Traffic, with 2 kWp (in orange) and 10 kWp (in blue) PV panel capacity, varying the number of BSs within the MG.

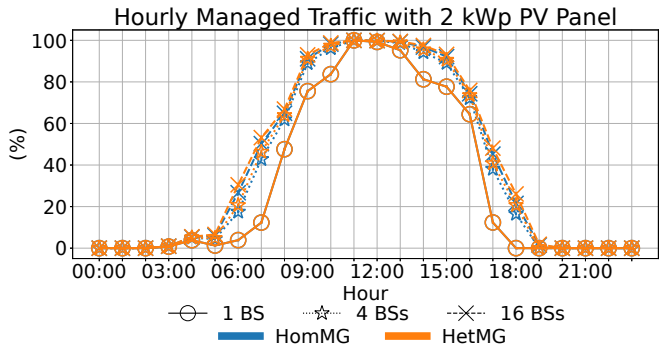

Fig. 8. Hourly Managed Traffic, with 2 kWp (in orange) and 10 kWp (in blue) PV panel capacity, varying the number of BSs within the MG, in the *HomMG* and *HetMG* scenarios.

three distinct areas. First, until 3:00 a.m. and after 20:00, the energy which is produced by the PV Panel is never sufficient, because of lack of energy production. Consequently, the PV Panel capacity or the number of BSs in the MG have no impact on the network resilience during these periods. Second, at 11:00 and 12:00, the portion of RAN is able to manage almost all the traffic demand, as the PV Panel always produces enough energy during these hours, regardless the PV panel capacity and/or how many BSs compose the MG. Finally, from 4:00 a.m. to 10 a.m. and between 13:00 and 20:00, the network performance is strictly related to the PV Panel capacity and/or the number of BSs in the MG. With 2 kWp, at 7:00 a.m., each single BS is able to manage 12% of the traffic demand (see orange curve, marked with circles), while with a MG composed of 4 and 16 BSs, the *Managed Traffic* reaches up to 50%.

B. Impact of the Traffic Patterns

In this part of the work, we analyse the performance during the PGOs in scenarios which differ for the heterogeneity of the traffic demand within the MG. In Fig. 8, the hourly *Managed traffic* is presented. The blue curves are the results for the *HomMG* scenario, i.e. where the BSs in the MG exhibit similar traffic demand profile, typical of scenario that operates under the assumption of load homogeneity in close geographical areas. The orange curves in the figure are for the *HetMG* scenario, characterized by MGs with BSs having dissimilar traffic demand shape. As mentioned in section III, this scenario reflects areas with heterogeneous loads within close geographical proximity, typical of areas with hotspots such as tourist attractions or parks. The curves denoted by

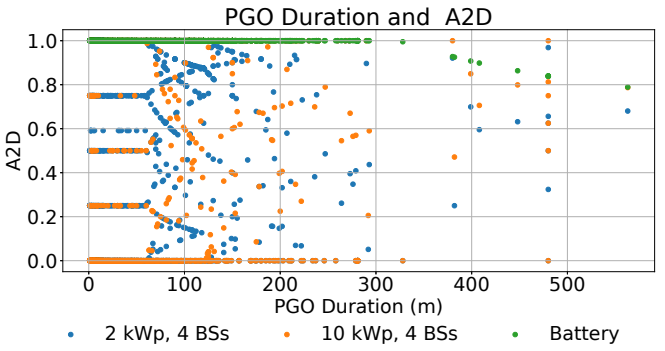

Fig. 9. *A2D* varying the PGO duration, in minutes.

the circles, starts and cross are the results in case the number of BSs in the MG is equal to 1, 4 and 16, respectively. When the MG is composed of a single BS, i.e. there is no energy exchange neither RAN resource management, the results obtained in the *HomMG* and *HetMG* scenarios are identical, as expected. For MG composed of 4 and 16 BSs, the situation is different. Until 5:00 a.m., after 7:00 p.m. and between 11:00 a.m. and 12 p.m., the *Managed Traffic* is identical, regardless of the scenario or number of BSs in the MG. This is due to the lack of energy generation during these time intervals or the large energy generation between 11:00 a.m. and 12:00 p.m., which is always sufficient for BS supply, as explained above (see Fig. 7). Between 6:00 a.m. and 10 a.m. and from 1 p.m. to 6 p.m., the figure shows that the heterogeneity of the traffic demand profiles of the BSs in the MG impacts the *Managed Traffic*. It is slightly larger (between 0.05% and 26%) in the *HetMG* scenario than in the *HomMG* one. This is because in the *HetMG* scenario, BSs have peaks and low traffic periods misaligned, making more likely energy exchange among the BSs.

C. Comparison with the Energy Battery as Back Up System

In this part of our study, we compare the performances obtained with the MG to the traditional solution, which involves using an energy battery with a capacity of 2.4 kWh as a backup system. We consider a maximum Depth of Discharge (DOD) of 70% for this battery. This DOD value allows the battery to operate for more than 500-600 cycles before needing replacement [31], [32]. Additionally, we account for losses of 25% in energy efficiency due to the charging and discharging processes [33]. Fig. 9 combines the PGO duration, in minutes, and the *A2D*, that is the fraction of time the BSs remain active relative to the PGO duration. Each PGO is represented with a marker positioned so that the x-axis value corresponds to the PGO duration and the y-axis value corresponds to the *A2D*, when that PGO occurs. In the figure, the blue and orange points are for the MG composed of 4 BSs, each equipped with a PV Panel system whose capacity is 2 kWp and 10 kWp, respectively; the green points are for the energy battery backup system solution. From Fig. 9, we notice that the PGO duration has no impact on the *A2D* in the MG. Indeed, as discussed in the previous sections, the performance is strictly dependent on the hour of the day, see Fig. 7. When an energy battery is employed as a backup system, the *A2D* is larger than when there is the MG. In this case, each BS remains active for almost the entire duration of the PGO. Nevertheless, as soon as the battery is depleted,

each BS turns off. This implies that the resulting performance is strictly dependent on the duration of the PGO. For PGOs longer than 300 minutes, the energy battery keeps a BS active for a shorter time than the MG cases, if the PGO occurs during daily hours.

D. Efficacy of the MG

In this section of the work, we formalize the lower bounds of the number of the MG loads (BSs) that should be included to improve the network resilience, related to the installed PV panel capacity. This occurs when, within the MG, at least a BS remains active during the PGO, i.e. the availability of sufficient renewable energy for its supply is met. For the sake of computational simplicity, we assume that each BS consumes the same amount of energy. The minimum achievement provided by the MG is maintaining active at least a single BS. This means that

$$E_{c,i}^{(t)} \leq \sum_{i=1}^{N} E_{p,i}^{(t)} \quad \text{for at least a BS } i \text{ in the MG} \qquad (2)$$

where N is the number of BSs within the MG, $E_{c,i}^{(t)}$ and $E_{p,i}^{(t)}$, in Wh, represent the energy consumption and production at time t for the i-*th* BS, respectively. We refer to a generic BS and we denote its energy consumption as $\tilde{E}_c^{(t)}$. Since the PV Panel of each BS belonging to the same MG produces equally, the total generated energy, equal to $\sum_{n=1}^{N} E_{p,n}^{(t)}$, can be formulated as $N\tilde{E}_p^{(t)}$, where $\tilde{E}_p^{(t)}$ is the energy production of the PV Panel at each BS in the MG, at time t. The generated energy at time t is computed as $E_p^{(t)} = \mathrm{K}\tilde{E}_p^{(t)}$, where $\tilde{E}_p^{(t)}$ is the energy generated by a unitary PV panel system (1 kWp) and *K* is the capacity of the PV panel system, in kWp. Consequently, the lower bound of the number of BSs in the MG is as follows:

$$N \geq \frac{E_c^{(t)}}{K\tilde{E}_p^{(t)}}, \quad \tilde{E}_p^{(t)} \neq 0, K \neq 0 \qquad (3)$$

This result relates the time-dependent energy consumption, consequently the time-dependent traffic load (see Eq. 1), and the time-dependent power supply. Their relationship is valuable for designing the PV Panel system of the RAN BSs and their interconnections for energy exchanges. When the inequality is met, the considered portion of the RAN can effectively adapt to electrical grid unavailability. This contributes to the resilience of the network during energy grid failures, in addition to the overall network sustainability. Properly sizing and configuring the PV Panel systems and their interconnections enhances the reliability and resilience of the energy supply, ensuring continuous and dependable operation even in challenging conditions.

V. Conclusion

In this work, we cope with the lack of energy provisioning from the power grid in the RAN, by treating the BSs as loads within a MG, equipped with PV Panels, that exchange energy through dedicated power cables. Our proposed RAN resource management is activated in case of PGOs and switches off BSs, until the energy produced within the MG becomes sufficient for supply. The results reveal that, although strictly dependent on the time of the day, our proposed methodology improves the experienced QoS, increasing the managed traffic up to 300%. Notably, achieved performances with PV Panels smaller than 6 kWp, when combined with the MG, are comparable to the ones obtained with 12 kWp PV Panels, making the solution feasible in terms of installation space requirements. Moreover, we demonstrate that the performance of our methodology is minimally influenced by the traffic demand profile of the BSs within the MG and entirely independent on the duration of PGOs. Finally, we formalize the relationship between the number of BSs in the MG and the required PV Panel capacity to ensure MG resilience. As the next steps of our work, we will compare our results with existing literature solutions, mathematically formalize the results, and evaluate the effects of BS parameters on performance, comparing the OPEX and the performance of our methodology with emergency solutions, such as drones equipped with BS hardware, to provide connectivity where PGO occurs and BSs can not be supplied, because of energy provisioning shortage.

Acknowledgment

This paper was supported by the European Union under the Italian National Recovery and Resilience Plan (NRRP) of NextGenerationEU, partnership on "Telecommunications of the Future" (PE00000001 - program "RESTART", Focused Project R4R).

References

[1] European Union Agency for Network and Information Security., "ENISA - Annual report telecom security incidents 2021." Tech. Rep. July, 2021.

[2] H. Jones, "Going beyond reliability to robustness and resilience in space life support systems." 50th International Conference on Environmental Systems, 2021.

[3] IEA. (2022) Unlocking the potential of distributed energy resources. IEA. License: CC BY 4.0. [Online]. Available: https://www.iea.org/reports/unlocking-the-potential-of-distributed-energy-resources

[4] ——. (2022) World energy outlook 2022. IEA. License: CC BY 4.0 (report); CC BY NC SA 4.0 (Annex A). [Online]. Available: https://www.iea.org/reports/world-energy-outlook-2022

[5] IEA. (2023) Global energy and climate model. https://www.iea.org/reports/global-energy-and-climate-model. IEA. Paris. License: CC BY 4.0.

[6] C. Marnay, S. Chatzivasileiadis, C. Abbey, R. Iravani, G. Joos, P. Lombardi, P. Mancarella, and J. Von Appen, "Microgrid evolution roadmap," in *2015 international symposium on smart electric distribution systems and technologies (EDST)*. IEEE, 2015, pp. 139–144.

[7] J. Shi, L. Ma, C. Li, N. Liu, and J. Zhang, "A comprehensive review of standards for distributed energy resource grid-integration and microgrid," *Renewable and Sustainable Energy Reviews*, vol. 170, p. 112957, 2022.

[8] N. Piovesan, D. López-Pérez, M. Miozzo, and P. Dini, "Joint load control and energy sharing for renewable powered small base stations: A machine learning approach," *IEEE Transactions on Green Communications and Networking*, vol. 5, no. 1, pp. 512–525, 2020.

[9] G. Vallero, D. Renga, M. Meo, and M. A. Marsan, "Greener ran operation through machine learning," *IEEE Transactions on Network and Service Management*, vol. 16, no. 3, pp. 896–908, 2019.

[10] G. Perin, M. Berno, T. Erseghe, and M. Rossi, "Towards sustainable edge computing through renewable energy resources and online, distributed and predictive scheduling," *IEEE Transactions on Network and Service Management*, vol. 19, no. 1, pp. 306–321, 2021.

[11] P. W. D. Bishop, S. J. Barrett, and I. D. Harris, "Managing projected power outage at mobile radio base sites," Jul. 16 2013, uS Patent 8,489,154.

[12] A. Cabrera-Tobar, F. Grimaccia, and S. Leva, "Energy resilience in telecommunication networks: A comprehensive review of strategies and challenges," *Energies*, vol. 16, no. 18, p. 6633, 2023.

[13] G. Vallero, E. Pristeri, and M. Meo, "Coping with power outages in mobile networks," in *2020 Mediterranean Communication and Computer Networking Conference (MedComNet)*. IEEE, 2020, pp. 1–4.

[14] J. P. Sterbenz, D. Hutchison, E. K. Çetinkaya, A. Jabbar, J. P. Rohrer, M. Schöller, and P. Smith, "Resilience and survivability in communication networks: Strategies, principles, and survey of disciplines," *Computer networks*, vol. 54, no. 8, pp. 1245–1265, 2010.

[15] A. Mauthe, D. Hutchison, E. K. Cetinkaya, I. Ganchev, J. Rak, J. P. Sterbenz, M. Gunkelk, P. Smith, and T. Gomes, "Disaster-resilient communication networks: Principles and best practices," in *2016 8th International Workshop on Resilient Networks Design and Modeling (RNDM)*. IEEE, 2016, pp. 1–10.

[16] Y. Xu, Y. Xing, Q. Huang, J. Li, G. Zhang, O. Bamisile, and Q. Huang, "A review of resilience enhancement strategies in renewable power system under hilp events," *Energy Reports*, vol. 9, pp. 200–209, 2023.

[17] Tim emilia romagna - alluvione. Gruppo TIM. [Online]. Available: https://www.gruppotim.it/it/gruppo/chi-siamo/news/TIM-EMILIAROMAGNA-ALLUVIONE.html

[18] H. Saboori, "Enhancing resilience and sustainability of distribution networks by emergency operation of a truck-mounted mobile battery energy storage fleet," *Sustainable Energy, Grids and Networks*, vol. 34, p. 101037, 2023.

[19] M. Deruyck, W. Joseph, E. Tanghe, and L. Martens, "Reducing the power consumption in lte-advanced wireless access networks by a capacity based deployment tool," *Radio Science*, vol. 49, no. 9, pp. 777–787, 2014.

[20] N. Piovesan, D. López-Pérez, M. Miozzo, and P. Dini, "Joint load control and energy sharing for renewable powered small base stations: A machine learning approach," *IEEE Transactions on Green Communications and Networking*, vol. 5, no. 1, pp. 512–525, 2020.

[21] J. Franceschi, J. Rothkop, and G. Miller, "Off-grid solar pv power for humanitarian action: from emergency communications to refugee camp micro-grids," *Procedia Engineering*, vol. 78, pp. 229–235, 2014.

[22] G. Castellanos, S. De Gheselle, L. Martens, N. Kuster, W. Joseph, M. Deruyck, and S. Kuehn, "Multi-objective optimisation of human exposure for various 5g network topologies in switzerland," *Computer Networks*, vol. 216, p. 109255, 2022.

[23] M. Matalatala, M. Deruyck, E. Tanghe, L. Martens, and W. Joseph, "Simulations of beamforming performance and energy efficiency for 5g mm-wave cellular networks," in *2018 IEEE Wireless Communications and Networking Conference (WCNC)*. IEEE, 2018, pp. 1–6.

[24] M. H. Nguyen and T. K. Saha, "Power loss evaluations for long distance transmission lines," in *Australian Geothermal Energy Conference*, 2009, pp. 307–312.

[25] G. Vallero, D. Renga, M. Meo, and M. Ajmone Marsan, "Processing ann traffic predictions for ran energy efficiency," in *Proceedings of the 23rd International ACM Conference on Modeling, Analysis and Simulation of Wireless and Mobile Systems*, 2020, pp. 235–244.

[26] A. A. per le Garanzie Nelle Comunicazioni, "OSSERVATORIO SULLE COMUNICAZIONI N.4/ 2018," AGCOM - Autorita per le Garanzie Nelle Comunicazioni, Tech. Rep. N.4/2018, 2018.

[27] ——, "OSSERVATORIO SULLE COMUNICAZIONI N.4/ 2023," AGCOM - Autorita per le Garanzie Nelle Comunicazioni, Tech. Rep. N.4/2023, 2023.

[28] A. P. Dobos, "Pvwatts version 5 manual," National Renewable Energy Lab.(NREL), Golden, CO (United States), Tech. Rep., 2014.

[29] M. I. Malinen and P. Fränti, "Balanced k-means for clustering," in *Structural, Syntactic, and Statistical Pattern Recognition: Joint IAPR International Workshop, S+ SSPR 2014, Joensuu, Finland, August 20-22, 2014. Proceedings*. Springer, 2014, pp. 32–41.

[30] M. Matalatala, M. Deruyck, S. Shikhantsov, E. Tanghe, D. Plets, S. Goudos, K. E. Psannis, L. Martens, and W. Joseph, "Multi-objective optimization of massive mimo 5g wireless networks towards power consumption, uplink and downlink exposure," *Applied Sciences*, vol. 9, no. 22, p. 4974, 2019.

[31] C. Mi and M. A. Masrur, *Hybrid electric vehicles: principles and applications with practical perspectives*. John Wiley & Sons, 2017.

[32] M. Jafari, G. Platt, Z. Malekjamshidi, and J. G. Zhu, "Technical issues of sizing lead-acid batteries for application in residential renewable energy systems," in *2015 4th International Conference on Electric Power and Energy Conversion Systems (EPECS)*. IEEE, 2015, pp. 1–6.

[33] H. Gharavi and R. Ghafurian, "Ieee recommended practice for sizing lead-acid batteries for stand-alone photovoltaic (pv) systems ieee std 1013–2007," in *Proc. IEEE*, vol. 99, no. 6, 2011, pp. 917–921.